Available online at www.sciencedirect.com
ScienceDirect
Journal of Power Sources 160 (2006) 1391–1394
JOURNAL OF POWER SOURCES
www.elsevier.com/locate/jpowsour

Short communication

Electrochemical properties of the $LaNi_{3.55}Mn_{0.4}Al_{0.3}Co_{0.4}Fe_{0.35}$ hydrogen storage alloy

M. Tliha [a,*], H. Mathlouthi [a], C. Khaldi [a], J. Lamloumi [a], A. Percheron-guegan [b]

[a] *Laboratoire de Mécanique, Matériaux et Procédés, ESSTT, 5 Avenue Taha Hussein 1008 Tunis, Tunisia*
[b] *Laboratoire de Chimie Métallurgique des Terres Rares, GLVT, 2-8 Rue Henri Dunant 94320, Thiais Cedex, France*

Received 19 October 2005; received in revised form 27 February 2006; accepted 9 March 2006
Available online 15 May 2006

Abstract

The electrochemical properties of $LaNi_{3.55}Mn_{0.4}Al_{0.3}Co_{0.4}Fe_{0.35}$ hydrogen storage alloy have been studied through chronopotentiometric, chronoamperometric and cyclic voltammogram measurements. The maximum capacity value obtained was 265 mAh g^{-1} at rate C/6 and the capacity decrease was recorded by 1.5% after 30 cycles. The values of the hydrogen diffusion coefficient D_H obtained through cyclic volammogram and chronoamperometric techniques were, respectively, 7.01×10^{-8} cm^2 s^{-1} and 4.23×10^{-11} cm^2 s^{-1}.

Keywords: Metal hydrides; Intermetallic compounds; Ploy-substituted; Hydrogen diffusion coefficient

1. Introduction

The Ni/MH batteries using hydrogen storage alloys as the negative electrode have several advantages over the conventional Ni/Cd secondary batteries; they have a higher specific energy density, a longer life, they are more resistant to over charge–discharge, and they are more compatible to the environment. Hence they are used quite extensively now [1–3]. However, the overall properties of Ni/MH batteries should be improved to face the competition of Li-ion batteries used for the personal computer, the mobile phone and the video cameras. The key to the improvement of the commercial Ni/MH batteries is the improvement of the electrochemical properties of the hydrogen storage alloys including the electrochemical capacity, the life cycle and the high rate of dischargeability.

Currently, two classes of metal-hydride alloys are being developed; a class of those based on rare earth metals (AB_5, where A represents a rare earth metal and B may include any of the late transition metals) [4–8] and another class involving alloys based on early transition metals (AB_2) [9–12].

Although the AB_2 alloys are reported to exhibit a higher specific energy than the AB_5 alloys, commercial Ni-MH batteries predominantly use AB_5 alloys. The AB_5 are based on $LaNi_5$ with various substitutes for La and Ni. The systematic effects of this alloy modification and the reasons for these effects, are current topics of research [13–17].

The beneficial effect of the substitutes for either La or Ni is often accompanied by an undesirable decrease in hydrogen absorption capacity and slow kinetics of hydrogen absorption and desorption. The performance of the metal-hydride electrode is determined by both the kinetics of the processes occurring at the metal/solution interface and the rate of hydrogen diffusion within the bulk of the alloy. In the present study, the electrochemical properties of the $LaNi_{3.55}Mn_{0.4}Al_{0.3}Co_{0.4}Fe_{0.35}$ hydrogen storage alloy have been studied.

2. Experimental

A hydrogen-storage alloy of the nominal composition $LaNi_{3.55}Mn_{0.4}Al_{0.3}Co_{0.4}Fe_{0.35}$ was prepared through the induction melting of the pure elements followed by an appropriate annealing to ensure a good homogeneity. The crystal structure of the alloy was examined by X-ray diffraction. The bulk chemical composition was analyzed by an electron probe microanalysis (EPMA). The so-called "latex" technology has been used for the electrode preparation [18]. The alloy is first ground and sieved (to less than 63 μm) in a glove box under argon

* Corresponding author. Tel.: +216 71496066; fax: +216 71391166.
E-mail address: Mohamed.Tliha@esstt.rnu.tn (M. Tliha).

0378-7753/$ – see front matter © 2006 Elsevier B.V. All rights reserved.
doi:10.1016/j.jpowsour.2006.03.026

Table 1
EPMA analysis, lattice parameters, cell volume of the compound $LaNi_{3.55}Mn_{0.4}Al_{0.3}Co_{0.4}Fe_{0.35}$

Compound	EPMA analysis	Cell parameters and volume		
		a (Å)	b (Å)	V (Å^3)
$LaNi_{3.55}Mn_{0.4}Al_{0.3}Co_{0.4}Fe_{0.35}$	$LaNi_{3.55}Mn_{0.40}Al_{0.28}Co_{0.40}Fe_{0.35}$	5.075	4.053	90.41

atmosphere. Ninety percent of this powder has been mixed with 5% of the carbon black (to obtain a good conductivity) and 5% of the polytetrafluorethylene (PTFE). Two pieces of 0.5 cm^2 of this latex have been pressed on each side of the nickel grid, playing the role of a current collector. All the electrochemical measurements were conducted at room temperature in a conventional three electrode open-air cell using a Voltalab 40 system (Radiometer Analytical) constituted by a Potentiostat-Galvanostat PGZ301.The electrolyte consisted of a 7 M KOH solution which was deaerated by a continuous flow of Argon through the cell. An Hg/HgO (7 M KOH) reference electrode was positioned close to the hydride-forming electrode in the working electrode compartment, while a nickel mesh counter electrode was placed in the second compartment of the cell. The working potential of the hydride forming the electrode was measured with respect to the Hg/HgO reference electrode. The electrode was cycled by galvanostatically charging at a C/6 rate up to 50% overcharge to ensure a complete charging of the hydride electrode and then a discharging at a D/6 for 30 cycles.

3. Results and discussion

3.1. Structural properties

The analysis of the alloy by an electron probe microanalysis (EPMA) have shown that this alloy is a single phase and has a homogenous composition in agreement with the nominal one (Table 1). The $LaNi_{3.55}Mn_{0.4}Al_{0.3}Co_{0.4}Fe_{0.35}$ compound crystallizes in the hexagonal $CaCu_5$ type structure with the lattice parameters given in Table 1.

3.2. Activation performance and discharge capacity

MH electrochemically absorbs and desorbs hydrogen in the alkaline solution as a reversible anode. The half cell reactions taking place in a MH_x/Ni battery may be written as follows:

$$MH_x + xOH^- \Leftrightarrow M + xH_2O + xe^- \quad (1)$$

$$Ni(OOH) + H_2O + e^- \Leftrightarrow Ni(OH)_2 + OH^- \quad (2)$$

Fig. 1 shows typical charge–discharge characteristic curves of the MH electrode. The longest discharge was seen in cycle 16 which lasted 4.5 h in C/6 rate. The cell was subjected to 30 cycles. During the charging at a C/6 rate for 9 h the cell acquired a voltage in the range −1 to −0.98 V. When discharging at a D/6 rate, the voltage dropped from −0.80 to −0.76 V. It can be seen in the figure that the plateau–time of the charge–discharge characteristics increased initially with the number of cycles. This

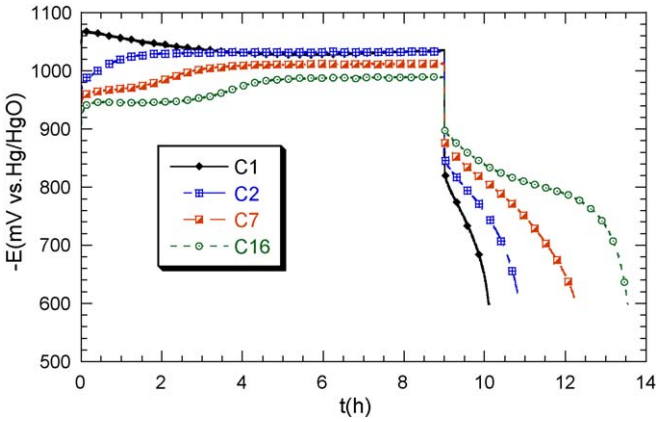

Fig. 1. Charge–discharge characteristics of $LaNi_{3.55}Mn_{0.4}Al_{0.3}Co_{0.4}Fe_{0.35}$ electrode of number of cycle.

seems to imply that the activation of the alloy surface occurred during the initial charge/discharge cycling.

The behaviour of the discharge capacity for the $LaNi_{3.55}Mn_{0.4}Al_{0.3}Co_{0.4}Fe_{0.35}$ negative electrode is shown as a function of the number of cycles in Fig. 2. The discharge capacity increases when increasing the number of the cycles, passing through a maximum at the 16th cycle (265 mAh g^{-1}). After 30 cycles the discharge capacity is lower by about 1.5% in comparison to its maximum value.

The evolution of the overpotential of the $LaNi_{3.55}Mn_{0.4}Al_{0.3}Co_{0.4}Fe_{0.35}$ alloy electrode as a function of the number of cycles is shown in Fig. 3. The potential increases by about 15 mV in the first 16 cycles and then remains constant when increasing the number of cycles. This drop in potential could be credited to the slower hydrogen transfer in the bulk of the alloy

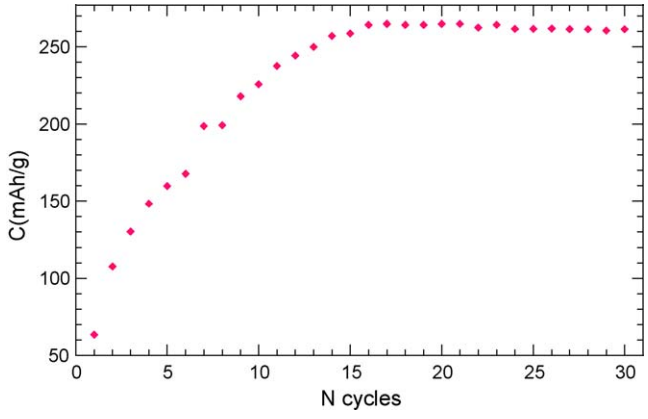

Fig. 2. Discharge capacity vs. cycle number for the $LaNi_{3.55}Mn_{0.4}Al_{0.3}Co_{0.4}Fe_{0.35}$ alloy electrode a 298 K.

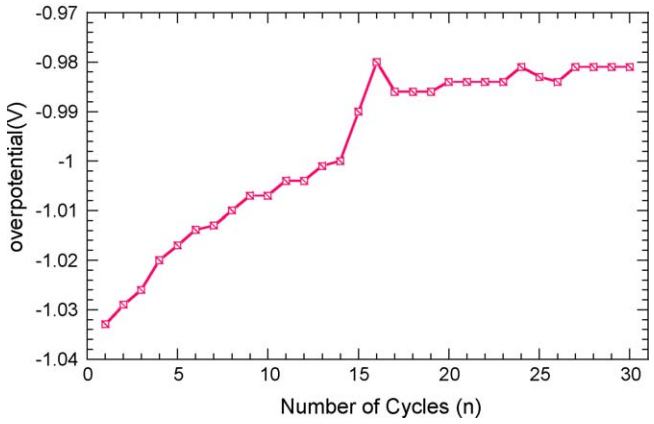

Fig. 3. Over potential of $LaNi_{3.55}Mn_{0.4}Al_{0.3}Co_{0.4}Fe_{0.35}$ alloy electrode with number of charge/discharge cycle.

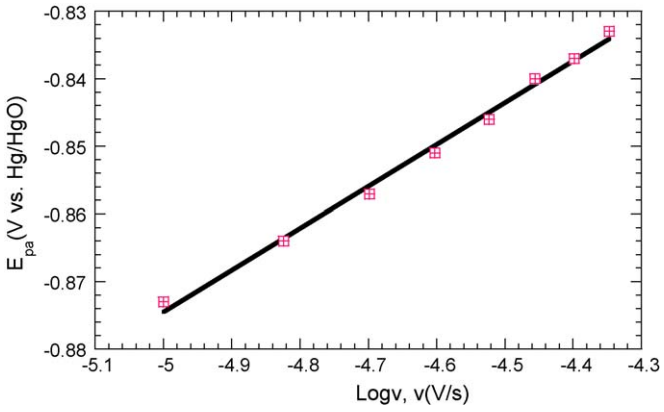

Fig. 5. Anodic peak potential of cyclic voltammogram of $LaNi_{3.55}Mn_{0.4}Al_{0.3}Co_{0.4}Fe_{0.35}$ electrode as function of log (v).

and the lower electrocatalytic activity at the surface during the first cycles.

3.3. Cyclic voltammograms

The cyclic voltammograms of the $LaNi_{3.55}Mn_{0.4}Al_{0.3}Co_{0.4}Fe_{0.35}$ electrode obtained at a various scan rate after the activation in the potential range of −0.5 to −1.1 V are shown in Fig. 4. The height of the oxidation/reduction peak shown in the figure reflects the kinetic property of the electrode and the peak area indicates the capacity of hydrogen absorption and desorption. The anodic current peak increases and its potential slightly shifts to the positive direction, increasing the potential scan rate.

The study of the variation of the peak discharge potential with potential sweep speed leads to the calculation of the slope $dE_{pa}/d(\log v) = 2.3RT/2\alpha nF$ which allows to determine the value of the transfer coefficient α. It can be seen also from Fig. 5, that the potential peak E_{pa} of the metal hydride electrode varies linearly with log (v).The value of the transfer coefficient α is estimated through the experiments to be 0.48 which allows us to conclude that the electrochemical reaction is reversible.

Fig. 6 presents the I_{pa} value as a function of the square root of the potential sweep rate ($V^{1/2}$) for MH electrode. The current of the oxidation peak (I_{pa}) of the voltammogram can be written [19] for a semi-infinite diffusion and an irreversible transfer in the form: $I_{pa} = 0.496\alpha^{1/2}(nF)^{3/2}SC_0[vD/RT]^{1/2}$. In our case, the geometrical surface of the working electrode is equal to 1 cm^2 and for the oxidation of the metal hydride, $n = 1$. The I_{pa} current is written then as: $I_{pa} = 2.98 \times 10^5 C_0 \alpha^{1/2} D^{1/2} v^{1/2}$, where C_0 is the concentration of the diffusing species (mol cm^{-3}), D the diffusion coefficient of the elector-active species (cm^2 s^{-1}) and v the scanning rate of the potential (V s^{-1}). The calculated slope $dI_{pa}/d\sqrt{v}$ allows to determine the value of the diffusion coefficient of hydrogen in the electrode of the alloy. The plot of I_{pa} vs. $v^{1/2}$ for the investigated electrode in Fig. 6 gives a straight line but without passing through the origin. This is somewhat different from literature [20,21]. Inoue [20] and Geng et al. [21] reported that the plot of I_{pa} vs. $v^{1/2}$ is a straight line passing through the origin, indicating that the oxidation of the absorbed hydrogen in the metal hydride electrode is controlled by the rate of the hydrogen diffusion in the bulk of the alloys and the slope of the straight line is proportional to the square root of the hydrogen diffusion coefficient. In the present case, the fact that the straight line is not passing through the origin may be due to the different electrode-preparation technique that needs to be studied further. The value of the diffusion coefficient in $LaNi_{3.55}Mn_{0.4}Al_{0.3}Co_{0.4}Fe_{0.35}$ measured by this method is 7.01×10^{-8} cm^2 s^{-1}.

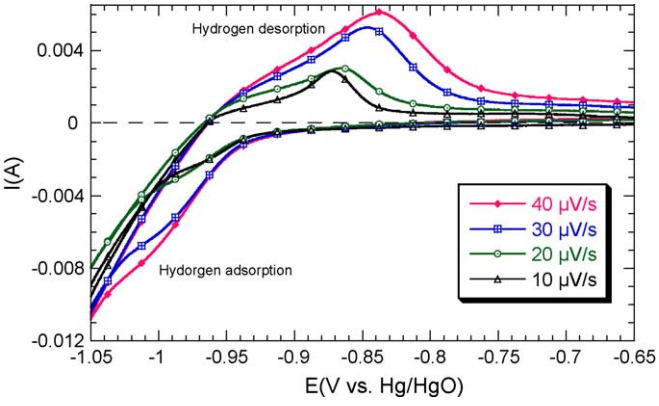

Fig. 4. Cyclic voltammograms of $LaNi_{3.55}Mn_{0.4}Al_{0.3}Co_{0.4}Fe_{0.35}$ electrode at various potential scan rate.

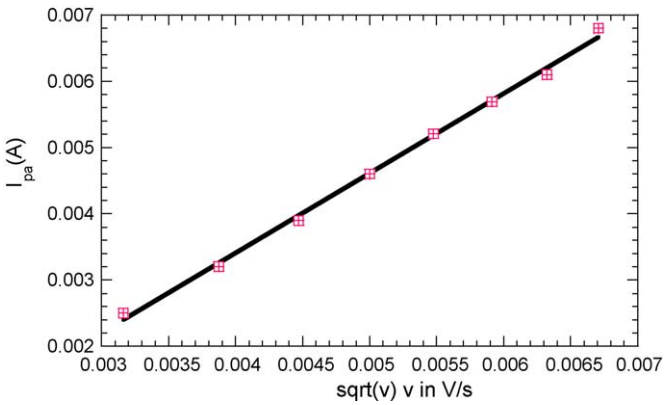

Fig. 6. Relationship between I_{pa} and $v^{1/2}$ for $LaNi_{3.55}Mn_{0.4}Al_{0.3}Co_{0.4}Fe_{0.35}$ electrode.

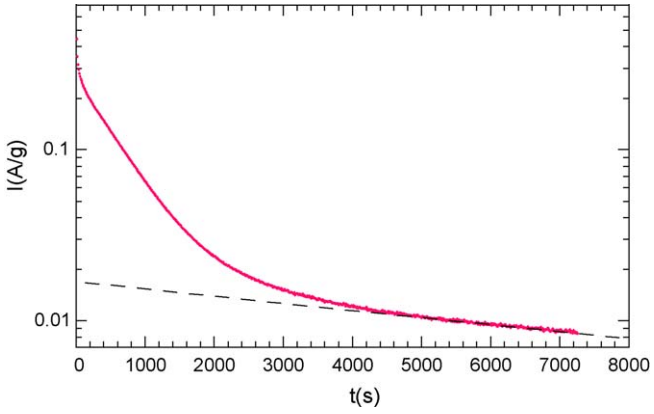

Fig. 7. Constant potential–discharge curve at $E = -0.6$ V vs. Hg/HgO and 100% state of charge.

3.4. Chronoamperometric experiments

Fig. 7 shows the semilograrithmic curve of the anodic current versus time response of the $LaNi_{3.55}Mn_{0.4}Al_{0.3}Co_{0.4}Fe_{0.35}$ alloy electrode. As shown in Fig. 7, the current response can be distinguished in two time regions. In the first time region, the current rapidly decreases due to a consumption of hydrogen on the surface. In the second time region, however, the current was slowly decreased in a linear way. Under this condition, hydrogen was supplied from the bulk of the alloy in a proportional way to the gradient concentration of hydrogen and the current was controlled by the diffusion of the hydrogen atom with time. According to a spherical diffusion model as proposed by Nishina et al. [22], the linear response in the second time region can be treated as the finite diffusion of hydrogen atom in the bulk of the alloy. In this case, Zhang et al. [23] considered that, for larger time, the hydrogen diffusion coefficient in the bulk of the alloy can be estimated through the slope of the linear region of the corresponding curve by the following equation:

$$\log i = \log\left(\frac{6FD}{da^2}(C_0 - C_s)\right) - \frac{\pi^2}{2.303}\frac{D}{a^2}t$$

where i, D, C_0, C_s, a, and t are the diffusion current density ($A\,g^{-1}$), the hydrogen diffusion coefficient ($cm^2\,s^{-1}$), the initial hydrogen concentration in the bulk of the alloy ($mol\,cm^{-3}$), the hydrogen concentration on the surface of the alloy particles ($mol\,cm^{-3}$), the alloy particle radius (cm), the density of the hydrogen storage alloy ($g\,cm^{-3}$), and the discharge time (s), respectively. From the slope of plot $\log i$ vs. t, D/a^2 may be evaluated, and if the sphere radius is known, the diffusion coefficient can be estimated. To satisfy the condition for a pure diffusion control, the fully charged electrode was discharged at a constant anodic potential of $E = -0.6$ V vs. Hg/HgO. A linear relationship was noticed between $\log i$ and t for the time longer than 5000 s, which is shown in Fig. 7. For the estimated average particle radius $a = 21$ μm [24], the effective diffusion coefficient of hydrogen through $LaNi_{3.55}Mn_{0.4}Al_{0.3}Co_{0.4}Fe_{0.35}$ alloy electrode was calculated to be $4.23 \times 10^{-11}\,cm^2\,s^{-1}$.

4. Conclusions

The hydrogen absorption capacity of the $LaNi_{3.55}Mn_{0.4}Al_{0.3}Co_{0.4}Fe_{0.35}$ alloy increases with the increase of the number of the cycles, passing through a maximum at the 16th cycle ($265\,mAh\,g^{-1}$). After 30 cycles the discharge capacity decreases by about 1.5% in comparison to its maximum value. The linear relationship was noticed between the anodic peak current density of voltammograms and the square root of the potential sweep rate. The diffusion coefficient of hydrogen through the alloy, estimated by cyclic voltammetry and chronoamperometry techniques is $7.01 \times 10^{-8}\,cm^2\,s^{-1}$ and $4.23 \times 10^{-11}\,cm^2\,s^{-1}$, respectively.

References

[1] T. Sakai, H. Miyamura, N. Kuriyama, A. Kato, K. Oguro, H. Ishikawa, J. Electrochem. Soc. 137 (1990) 795.
[2] C.S. Wang, Y.Q. Lei, Q.D. Wang, Electrochim. Acta 43 (1998) 3193.
[3] J.J.G. Willems, Philips J. Res. 39 (1) (1984) 1.
[4] J.J.G. Willems, K.H.J. Buschow, J. Less-Comm. Metals 129 (1987) 13.
[5] T. Sakai, H. Yoshinaga, H. Miyamura, H. Ishikawa, J. Alloys Comp. 180 (1992) 37.
[6] P.H.L. Notten, R.E.F. Einerchard, Adv. Matter 3 (1991) 1.
[7] T. Sakai, H. Miyamura, N. Kuriyama, A. Kato, K. Oguro, H. Ishikawa, C. Iwakura, J. Less-Comm. Metals 159 (1990) 127.
[8] T. Sakai, H. Miyamura, N. Kuriyama, H. Ishikawa, I. Uehara, J. Alloys Comp. 192 (1993) 155.
[9] H. Cunmao, H. Degang, L. Qiozlu, J. Less-Comm. Metals 172 (1991) 1044.
[10] Y. Moriwaki, T. Gano, T. Iwaki, J. Less-Comm. Metals 172 (1991) 1028.
[11] F.J. Lin, S. Suda, G. Sandrok, J. Alloys Comp. 232 (1996) 232.
[12] G. Xueping, S. Deying, Z. Yunshi, W. Genshi, S. Panwen, J. Alloys Comp. 223 (1995) 77.
[13] T. Gano, Y. Moriwaki, N. Yanagihara, T. Iwaki, J. Less-Comm. Metals 89 (1983) 495.
[14] A.P. Guegan, C. Lartigue, J.C. Achard, J. Less-Comm. Metals 109 (1985) 287.
[15] E.L. Huston, G.D. Sandrok, J. Less-Comm. Metals 74 (1980) 435.
[16] M. Cineranu, D.H. Ryanad, J.O. Stron-Olsen, J. Electrochem. Soc. 140 (1993) 579.
[17] N.J. Pilkington, J. Less-Comm. Metals 161 (1990) 1044.
[18] H. Mathlouthi, J. Lamloumi, M. Latroche, A. Percheron-Guégan, Ann. Chim. Sci. Mat. 22 (1997) 241.
[19] H. Matsuda, Y. Ayabe, Z. Electrochem. 59 (1955) 494.
[20] H. Inoue, M. Miyamoto, M. Matsuoka, Y. Fukumoto, C. Iwakura, Electrochim. Acta 42 (1997) 1087.
[21] M.M. Geng, J.W. Han, F. Feng, D.O. Northood, J. Electrochem. Soc. 146 (1999) 3591.
[22] T. Nishina, H. Ura, I. Uchida, J. Electrochem. Soc. 144 (1997) 1273.
[23] G. Zhang, B.N. Popov, R.E. White, J. Electrochem. Soc. 142 (1995) 2695.
[24] J.-M. Joubert, M. Latroche, R. Cerny, A. Percheron-Guégan, K. Yvon, J Alloys Compd. 330–332 (2002) 208–214.